Direct Formation of Acetaldehyde from Ethane Using Carbon Dioxide as a Novel Oxidant over Oxidized Diamond-Supported Catalysts

Kimito Okumura,[†] Kiyoharu Nakagawa,[†,‡] Takahiro Shimamura,[†] Na-oki Ikenaga,[†] Mikka Nishitani-Gamo,[§] Toshihiro Ando,[‡] Tetsuhiko Kobayashi,[||] and Toshimitsu Suzuki*[,†]

Department of Chemical Engineering and High Technology Research Center, Kansai University, Suita, Osaka 564-8680 Japan, National Institute for Material Science (NIMS) 1-1, Namiki, Tsukuba, Ibaraki 305-0044, Japan, Department of Applied Chemistry, Faculty of Engineering, Toyo University, 2100, Kujirai, Kawagoe, Saitama 350-8585, Japan, and Special Division for Green Life Technology, National Institute of Advanced Industrial Science and Technology (AIST), Ikeda, Osaka 563-8577, Japan

Received: May 28, 2003; In Final Form: September 23, 2003

We have developed a novel method of producing acetaldehyde directly from ethane using carbon dioxide. The selective oxidation of C_2H_6 using CO_2 as an oxidant was studied over various metal oxide-loaded catalysts. Among metal oxides, vanadium oxide afforded the highest activity toward CH_3CHO when it was loaded on the oxidized diamond. With a V_2O_5 loading level of 3 wt % on oxidized diamond, 140 μmol/h·g of catalyst of CH_3CHO was obtained at 923 K with C_2H_6 and CO_2 (1:1 mixed gas) in SV of 18 000 mL/h·g of catalyst. C_2H_4 and HCHO were obtained as byproducts. In the absence of CO_2, no aldehydes were obtained, indicating that oxygen was supplied from CO_2 through the vanadium oxide surface.

1. Introduction

The direct formation of oxygenates from alkane and oxygen is one of the goals of catalyst development. The selective oxidation of light alkanes to oxygenates has been investigated.[1−15] Oyama and Somorjai reported that a small amount of CH_3CHO is formed as a byproduct of C_2H_4 formation in the reaction between C_2H_6 and O_2 over silica and silica-supported vanadium oxide.[1] Kobayashi et al. have reported that silica supported with a very small amount of iron (Fe/Si = 0.05% in atomic ratio) afforded the selective formation of HCHO from CH_4 and O_2 at a conversion of methane lower than 1%.[2,3] More recently, they have found that the addition of alkali metal ions to Fe/SiO_2 catalysts can appreciably enhance the formation of CH_3CHO and acrolein in the reaction between C_2H_6, C_3H_8, and O_2.[6−11] However, in most reports, the selectivity to CH_3CHO was low (<30%) when O_2 was used as an oxidant. Such difficulties in the formation of oxygenates are due mainly to the weaker stability of the products than that of C_2H_6, allowing the overoxidation of oxygenates to proceed. N_2O was used as an oxidant, and it was believed to be a more selective oxidant than O_2 in C_2H_6 oxidation.[16−24]

$$C_2H_6 + O_2 \rightarrow CH_3CHO,\ CH_3COOH \qquad (1)$$

We have first found that CO_2 markedly promoted the dehydrogenation of C_2H_6 over Ga_2O_3-based catalysts with high selectivity to give C_2H_4 as shown in reaction 2.[25−27] Recently, CO_2 has been used by several researchers as a mild oxidant for the dehydrogenation of hydrocarbons.[28−32] The advantage of CO_2 as an oxidant seems to lie in its prevention of the overoxidation of alkane and alkene to give carbon oxides. As a result, a high yield and selectivity of C_2H_4 would be expected.

$$C_2H_6 + CO_2 \rightarrow C_2H_4 + CO + H_2O \qquad \Delta H^0_{298} = +134\ \text{kJ/mol} \quad (2)$$

The oxidation capability of CO_2 was first reported by some of us for the V_2O_5/MgO catalyst in the dehydrogenation of ethylbenzene, where CO_2 might have kept vanadium oxide in a higher oxidation state.[31,32] In addition, the redox cycle of Fe_3O_4 and Fe_3O_{4-x} with CO_2 in the dehydrogenation of ethylbenzene has been reported previously.[30] These findings lead us to exploit the use of CO_2 as an oxidant of hydrocarbon to oxygenates (reaction 3).

$$C_2H_6 + 2CO_2 \rightarrow CH_3CHO + 2CO + H_2O \qquad \Delta H^0_{773} = +195\ \text{kJ/mol} \quad (3)$$

No sp^3-hybridized carbon materials have been used as catalyst supports. Recently, we were the first to find that oxidized powdered diamond exhibited excellent behavior in the catalyst support.[33−38] The oxidized diamond surface may be considered to be a pseudo solid carbon oxide phase, which may have characteristics similar to silica, which is in the same group of elements as carbon. The advantage of using an oxidized diamond supported catalyst seems to be a weak interaction between the supported metal or metal oxide and the oxidized diamond. In light of this, we have exploited the selective oxidation of C_2H_6 with CO_2 using an oxidized diamond supported catalyst.

2. Experimental Section

2.1. Preparation of Catalysts. Catalysts were prepared by means of the impregnation method. As support materials, SiO_2

* Corresponding author. E-mail: tsuzuki@ipcku.kansai-u.ac.jp. Tel: +81-6-6368-0865. Fax: +81-6-6388-8869.
[†] Kansai University.
[‡] National Institute for Material Science (NIMS) 1-1.
[§] Toyo University.
[||] National Institute of Advanced Industrial Science and Technology (AIST).

10.1021/jp0354797 CCC: $25.00
Published on Web 11/11/2003

(Fuji Silysia Chemical Ltd., Q-30, surface area (SA) = 110 m^2/g), MgO (Ube Industries, Ltd., SA = 144 m^2/g), Al_2O_3 (JRC-ALO-4, SA = 149 m^2/g), Nb_2O_5 (Nacalai tesque, SA = very small), TiO_2 (Japan Aerosil Co., SA = 47m^2/g), Ta_2O_5 (Mitsuwa Chemicals SA = very small), GeO_2 (Kishida Chemicals, SA = very small), SnO_2 (Wako Pure Chemical Industries Ltd., SA = very small), and fine-powdered diamond (General Electric Company, SA = 20 m^2/g) were used. Metal oxides were impregnated into a support material by immersion into an aqueous solution of metal ions and leaving to stand overnight; after the removal of excess water, the mixture was calcined at 873 K in air for 5 h, though oxidized diamond support calcinations were carried out at 723 K. For vanadium and molybdenum sources, oxyammonium salts (NH_4VO_3 and $(NH_4)_6Mo_7O_{24}\cdot 4H_2O$ (Wako Pure Chemical Industries Ltd.)) were employed.

Oxidized diamond was prepared as reported previously.[33−38] Commercial powdered diamond was hydrogenated at 1173 K for 1 h under a pure H_2 stream. This thermal treatment gives species containing a C−H structure on the diamond surface. The hydrogenated diamond powder was then oxidized at 723 K for 5 h under an O_2 stream (O_2/Ar = 1:4). The oxidized diamond powder has a specific surface area of 12.6 m^2/g.

2.2. Characterization. Fourier transform infrared (FT-IR) spectra were obtained using a JEOL JIR 7000 instrument in diffuse reflectance mode. UV−vis spectra were recorded on a JASCO V560 in diffuse reflectance mode. Both IR and UV spectra were corrected using the Kubelka−Munk function.

The surface area was determined using the BET method (N_2 adsorption at 77 K) employing a Micromeritics Gemini model 2375 instrument.

2.3. Catalytic Reaction. The catalytic reactions were performed in a fixed-bed continuous flow reactor (quartz tube with 8-mm i.d. and 140-mm length) at atmospheric pressure. The catalyst was placed in the center of the reactor tube in the presence of quartz wool. The catalyst (100 mg) and a sheathed thermocouple were positioned at the hottest area of the reactor. The reaction temperature was measured and controlled by this thermocouple and was set between 773 and 973 K. A reaction gas mixture consisting of 50 vol % C_2H_6 and 50 vol % CO_2 was introduced at a feed rate of 30 mL/min. The reactants and products were analyzed by using an on-line gas chromatograph that consisted of a microgas chromatograph equipped with a TCD (CP2002, GL Science Co.) and two columns (CP-sil and Hysep A). The conversion of C_2H_6 was calculated on the basis of the area of C_2H_6 fed and recovered using precalibrated results.

3. Results and Discussion

3.1. Diffuse Reflectance FT-IR Spectroscopic Analysis of Hydrogenated and Oxidized Diamonds. Figure 1 shows the diffuse reflectance FT-IR spectra of hydrogenated diamond and oxidized diamond. Scheme 1 shows the model of hydrogenated diamond and oxidized diamond. The spectrum of hydrogenated diamond contained bands in the region of 2800−2970 cm^{-1}, which were ascribed to C−H stretching vibrations (ν_{C-H}) of sp^3-hybridized bonding.[39−42] Oxidized diamond was obtained by the oxidation of hydrogenated diamond at 723 K for 1 h under a stream of O_2/Ar (1:4 mixture). No significant C−H stretching vibrations were observed on the oxidized diamond. The spectrum of oxidized diamond contained bands in the region of 1650−1850 cm^{-1}, which were ascribed to C═O stretching vibrations (νC═O), and absorptions at 1250 cm^{-1} were assigned to C−O−C stretching vibrations (νC−O).[39−42] These results indicated that oxygen species were introduced into the diamond surface.

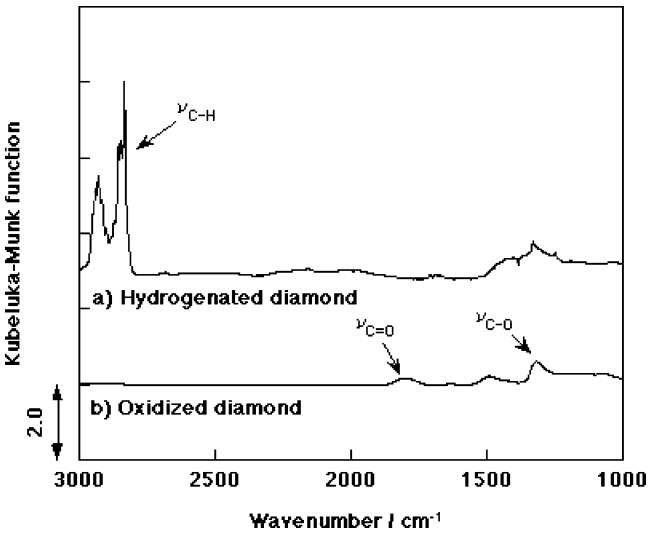

Figure 1. Diffuse reflectance FT-IR spectra of hydrogenated diamond (a) and oxidized diamond (b).

SCHEME 1

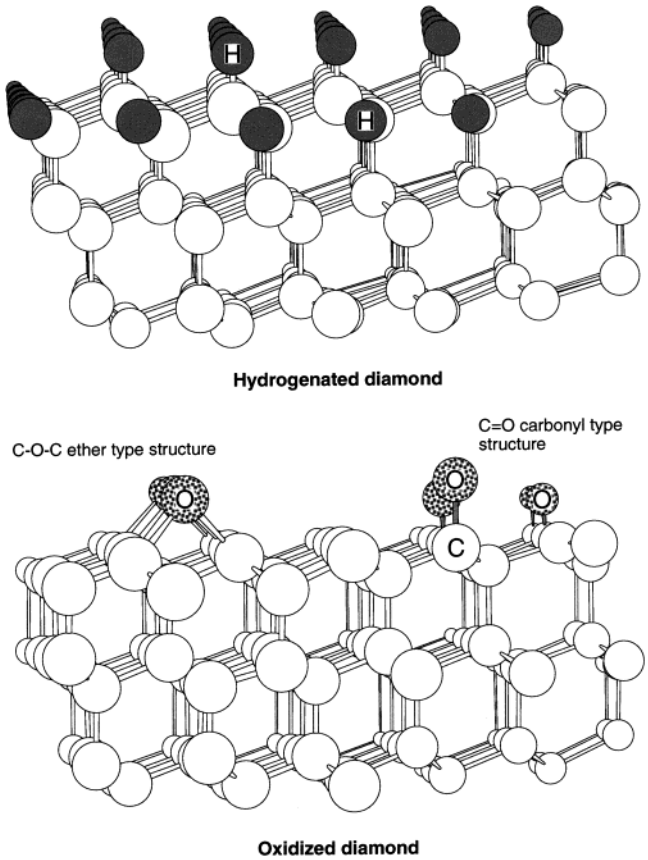

3.2. Catalytic Behavior of Metal Oxide-Loaded Catalysts in the Oxidation of Ethane Using CO_2. Oyama et al. reported that pure silica could catalyze the oxidative dehydrogenation of C_2H_6 with O_2 to give C_2H_4 together with a trace amount of CH_3CHO.[1] Until now, no report has been published regarding the selective oxidation of C_2H_6 to oxygenates using CO_2 as an oxidant. Table 1 shows results of the selective oxidation of C_2H_6 using CO_2 over various silica-supported metal oxides. Only vanadium and molybdenum oxides exhibited catalytic activity for this reaction, and the highest oxygenate yield was obtained using the vanadium-loaded catalyst. When the vanadium oxide-loaded catalyst was used, CO_2 exhibited an oxidation capability similar to that of O_2 or N_2O as an oxidant for the selective

TABLE 1: Catalytic Performance of M/SiO_2 in the Oxidation of Ethane[a]

M/SiO_2	temp[b] 1/K	C_2H_6 conv %	yield/μmolh^{-1} CH_3CHO	HCHO	C_2H_4	CO
none (SiO_2)	773		0.0	0.0	0	20
Fe	923		0.0	0.0	20	70
Mo	823	2.4	1.5	0.0	0	20
V	923	3.0	2.7	0.0	120	600

[a] Catalyst = 100 mg, SV = 18 000 mL h^{-1} g of catalyst^{-1}. C_2H_6/CO_2 = 5:25 mL/mL. Total flow rate = 30 mL/min. [b] Reaction temperature obtained at the maximum yield of CH_3CHO.

TABLE 2: Effect of Various Supports on the Conversion of C_2H_6 to CH_3CHO over Various Vanadium Oxide-Loaded Catalysts[a]

		yield/μmol h^{-1}			
		CO_2 flow		Ar flow	
V_2O_5/support	temp/K	CH_3CHO	C_2H_4	CH_3CHO	C_2H_4
MgO	973	0.0	1400		
Al_2O_3	973	0.0	2500	0.0	3000
Nb_2O_5	773	0.2	0	0.0	800
TiO_2	873	0.7	20		
Ta_2O_3	923	0.9	100	0.0	1700
Ge_2O_3	773	1.6	0	0.0	900
SnO_2	873	3.2	3	0.0	1400
SiO_2	973	5.6	1500	0.0	1900
O-dia	923	14.1	180	0.0	1200

[a] Catalyst: loading level 3 wt %; 100 mg. SV: 18 000 mL h^{-1} g-cat^{-1}; total flow rate, 30 mL min^{-1}, C_2H_6/CO_2 (or Ar) = 15:15 mL/mL.

oxidation reaction of C_2H_6. Iron oxide-loaded silica did not give an aldehyde, but a small amount of C_2H_4 was obtained. Although only a trace amount of aldehyde was produced over the Mo-loaded silica catalyst, the deactivation of the catalyst occurred rapidly.

The effects of various supports on the oxidation of C_2H_6 in the presence or absence (under Ar flow) of CO_2 over the vanadium oxide-loaded catalyst were examined. The results are summarized in Table 2. The optimal reaction temperatures giving the highest yield of CH_3CHO on the respective catalysts under the experimental conditions are shown in this Table. The major products of the reaction are C_2H_4, CO, and CH_3CHO. As seen in Table 2, the performance of supported vanadium oxide catalysts depended strongly upon the support oxides. MgO and Al_2O_3 exhibited high catalytic activity for the dehydrogenation of C_2H_6; however, no oxygenates were obtained. Vanadium oxide supported on Nb_2O_5, TiO_2, and Ta_2O_5 produced very small amounts of acetaldehyde, but the catalytic activities were very poor. GeO_2, SiO_2, and oxidized diamond supports in group 14 metal oxides and SnO_2 showed higher activity in comparison to other supports. SiO_2 and oxidized diamond yielded a considerable amount of CH_3CHO together with the dehydrogenation of C_2H_6 to C_2H_4. Particularly, vanadium oxide-loaded oxidized diamond exhibited the highest catalytic activity among these supports. The sum of the yields to aldehydes (HCHO and CH_3CHO) was 16 μmol/h. In addition, a loss of catalytic activity did not occur, which was observed during the reaction on all other vanadium oxide-loaded catalysts. The turnover rate in the oxidation of C_2H_6 over this catalyst is calculated to be 1.2 h^{-1}/V_2O_5 at a reaction temperature of 923 K.

To test the possibility of oxygen transfer from the lattice oxygen of vanadium oxide to C_2H_6, C_2H_6 and CO_2 flow were switched to a C_2H_6 and Ar mixture. CH_3CHO disappeared immediately on all of the vanadium oxide-loaded catalysts when the CO_2 supply was terminated. This clearly indicates that the selective oxidation of C_2H_6 proceeds in the presence of CO_2, suggesting that CO_2 acts as an oxidant.

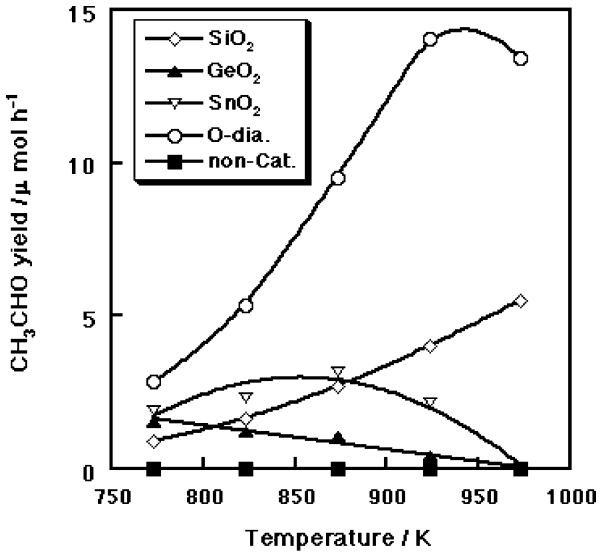

Figure 2. Effect of temperature on CH_3CHO yield in the group 14 metal oxide-supported V_2O_5 catalysts. C_2H_6/CO_2 = 15:15 mL/mL, flow rate = 30 mL/min. Catalyst = 100 mg, SV = 18 000 mL h^{-1} g of catalyst^{-1}. V_2O_5 loading level = 2 wt %.

Figure 2 shows the effect of reaction temperature on the yield of CH_3CHO for group 14 metal oxide-supported vanadium oxide catalysts. On these supports, the CH_3CHO yield increased with an increase in the reaction temperature, and above 923 K it decreased except in the SiO_2-supported case. V_2O_5-loaded oxidized diamond passed through the maximum yield of CH_3CHO (14 μmol/h) at a temperature of 923 K. The homogeneous conversion of C_2H_6 (i.e., the reaction of C_2H_6 and CO_2 in the absence of catalysts) did not occur, and no acetaldehyde was produced in the reaction-temperature range examined. This indicates that the contribution of homogeneous reactions in the gas phase to the catalytic process can be neglected under the experimental conditions of this work.

3.3. Effect of Reaction Conditions over the V_2O_5/O-Diamond Catalyst. Among the various supports shown in Table 2 and Figure 2, the oxidized diamond supported catalyst afforded the highest CH_3CHO yield. The effect of the loading level of vanadium oxide on the oxidized diamond support was examined at 923 K. The results are illustrated in Figure 3. The highest yield of CH_3CHO was obtained at 3 wt % V_2O_5, but the C_2H_4 yield increased with an increase in the loading level of V_2O_5. Without V_2O_5, bare oxidized diamond itself produced a trace amount of C_2H_4 but no CH_3CHO. These results indicate that both V_2O_5 and oxidized diamond affected the formation of CH_3CHO and the decomposition of CH_3CHO to give C_2H_4 and CO.

With 3 wt % V_2O_5-loaded oxidized diamond as seen in Figure 4, the effect of the CO_2 partial pressure on the yield of CH_3CHO and C_2H_4 was examined over the V_2O_5-loaded oxidized diamond catalyst. The reactions were carried out at a constant C_2H_6 partial pressure by diluting CO_2 with Ar. No aldehydes were produced under Ar flow in the absence of CO_2. However, the CH_3CHO yield markedly increased when the CO_2 partial pressure increased. In contrast, the C_2H_4 yield exhibited a maximum in the absence of CO_2 and decreased slightly with an increase in the CO_2 partial pressure. These results strongly suggest that CO_2 plays an important role in the formation of CH_3CHO. However, the formation of C_2H_4 was suppressed by CO_2 over the V_2O_5-

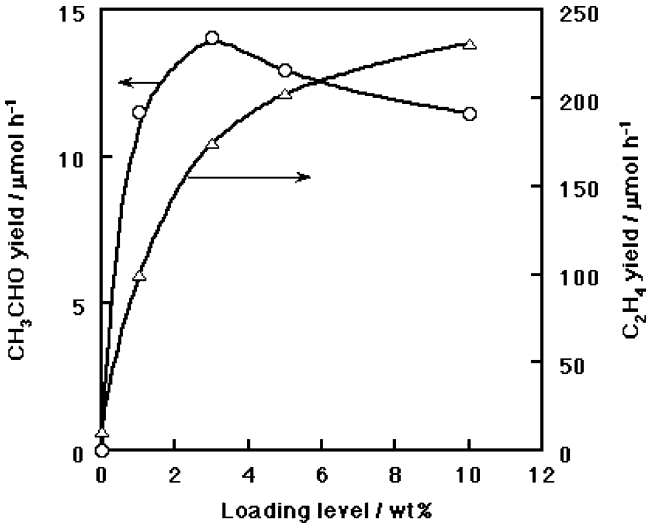

Figure 3. Effect of loading level of V_2O_5−diamond on CH_3CHO and C_2H_4 yields. C_2H_6/CO_2 = 15:15 mL/mL, flow rate = 30 mL/min, catalyst = 100 mg. SV = 18 000 mL h^{-1} g of catalyst^{-1}, reaction temperature = 923 K.

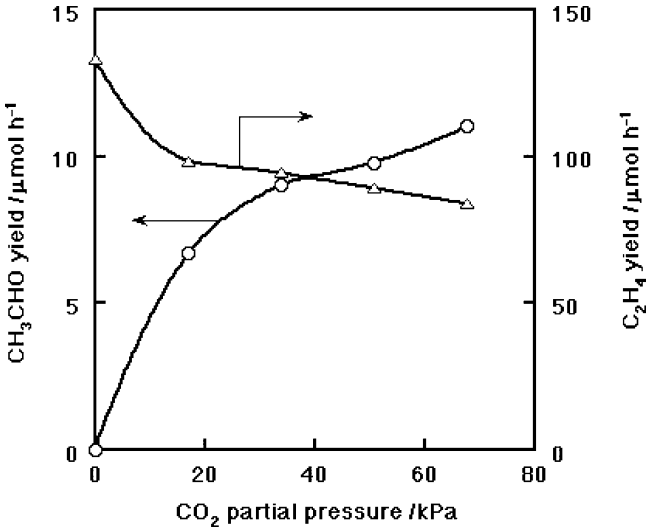

Figure 4. Effect of CO_2 partial pressure on CH_3CHO and C_2H_4 yields over V_2O_5/O-diamond. Temperature = 923 K, SV = 18 000 mL h^{-1} g of catalyst^{-1} C_2H_6 = 10 mL/min, total flow rate = 30 mL/min, catalyst = 100 mg.

loaded oxidized diamond catalyst. This is quite different behavior from the dehydrogenation of C_2H_6 over the Cr_2O_3-loaded oxidized diamond catalyst, where dehydrogenation in the presence of CO_2 was enhanced to a degree 3 times that of Ar flow in the absence of CO_2.[33,37] In the C_2H_6−CO_2 reaction, the product is strongly affected by the loaded metal oxide species on the oxidized diamond supported catalyst; therefore, the support effect of oxidized diamond seems to be quite apparent.

Figure 5 shows the effect of space velocity (SV) on the CH_3CHO and HCHO yields over the V_2O_5-loaded oxidized diamond catalyst at a reaction temperature of 923 K. SV was varied by changing the feed rate of the C_2H_6 and CO_2 mixture. In general, in almost all the catalytic reactions, an increase in the SV (i.e., a decease in the contact time between the reactant and catalyst) afforded decreases in the product yields. In contrast, in the selective oxidation of C_2H_6 to oxygenates using CO_2, the CH_3CHO yield increased with an increase in the SV. In proportion to the increase in the CH_3CHO yield, the HCHO yield increased, and larger amounts of CH_4 and CO were obtained. These observations suggest that HCHO is formed

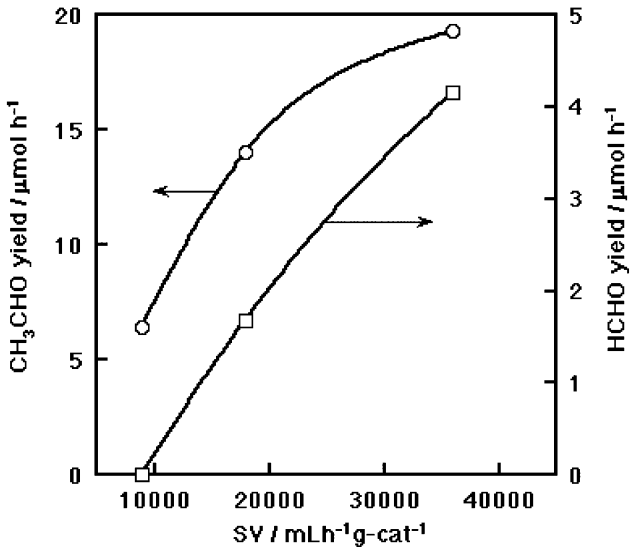

Figure 5. Effect of SV on CH_3CHO and HCHO yields over V_2O_5 (3 wt %)/O-diamond. C_2H_6/CO_2 = 1:1, catalyst = 100 mg, temperature = 923 K.

through the decomposition of CH_3CHO (eq 4). A part of HCHO formed from CH_3CHO further decomposed into CO and H_2 (eq 5). A certain amount of CH_3CHO seems to decompose also into CH_4 and CO (eq 6). Thus, the inverse behavior of CH_3CHO yield versus SV is ascribed to the decomposition of the product, and during the longer contact time, CH_3CHO decomposed to give undesired byproducts at a high temperature.

$$CH_3CHO \rightarrow HCHO + C1 \text{ products} \quad (4)$$

$$HCHO \rightarrow CO + H_2 \quad (5)$$

$$CH_3CHO \rightarrow CH_4 + CO \quad (6)$$

3.4. Infrared and UV−Vis Absorption Spectra of the V_2O_5-Loaded Oxidized Diamond Catalyst. To obtain more information regarding the role of CO_2 in the oxidation of C_2H_6 and the catalytic active species over the V_2O_5-loaded oxidized diamond catalyst, fresh and reacted catalysts were analyzed using IR and UV−vis spectra. Results of IR measurements are shown in Figure 6. The bands at 840 and 1020 cm^{-1} are ascribed to the V═O stretching and V−O−V bending vibrations from V_2O_5, respectively.[43−46] The two absorption bands near 1790 and 1300 cm^{-1} are the characteristic bands assigned to the vibrations of νC═O and νC−O−C on oxidized diamond surfaces.[39−42] After the selective oxidation of C_2H_6, the relative intensities of all of these absorptions on V_2O_5-loaded oxidized diamond decreased as compared to those observed for the fresh catalyst. However, all of these bands disappeared after the reaction of C_2H_6 in Ar. These results indicate that the lattice oxygen of vanadium oxide (V═O and/or V−O−V) and the oxygen on the diamond surface (C═O and/or C−O−C) transfer to C_2H_6 to give oxygenates and that oxygen atoms on the solid surface were lost. Only a small portion of oxygen on vanadium oxide was supplied from gas-phase CO_2. The CH_3CHO formation rate slightly decreased during a prolonged run, but the initial activity was maintained for more than 2 h. This indicates that only a small number of surface oxygens of vanadium oxide on oxidized diamond might have retained their catalytic activity. A new and weak absorption at 2900 cm^{-1} appeared on V_2O_5-loaded oxidized diamond catalysts after the reaction of C_2H_6 in both the presence and absence of CO_2, which is associated with the C−H stretching vibration on oxidized diamond surfaces.[39]

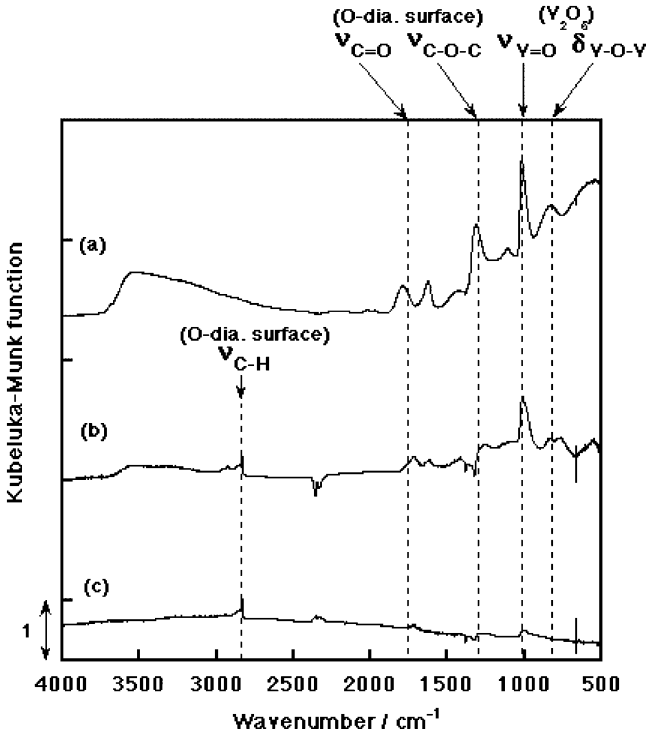

Figure 6. Diffuse reflectance FT-IR spectra of V_2O_5/O-diamond. (a) V(3 wt %)/O-diamond fresh catalyst. (b) V(3 wt %)/O-diamond after oxidation of ethane with CO_2 at 923 K for 1 h. (c) V(3 wt %)/O-diamond after reaction of ethane with Ar at 923 K for 1 h.

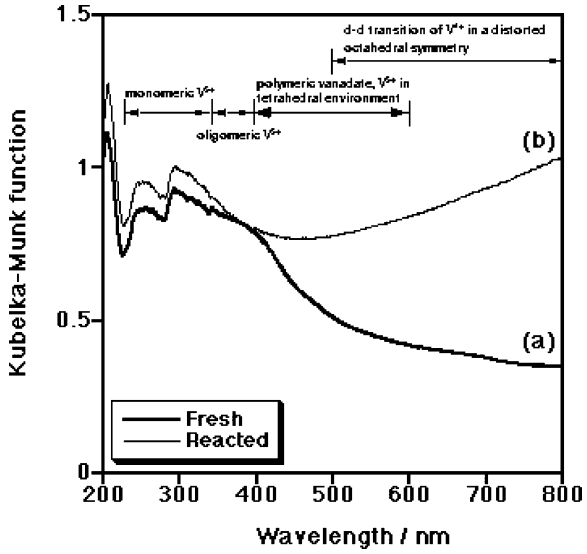

Figure 7. UV−vis spectra of fresh and reacted V/O-diamond catalysts. (a) V/O-diamond fresh catalyst. (b) V/O-diamond after oxidation of ethane with CO_2 at 923 K for 1 h.

The C−H bond is considered to have formed on the diamond surface through the hydrogen transfer from H_2 produced in the dehydrogenation of C_2H_6.

To understand the valence state of the vanadium species in the vanadium oxide on oxidized diamond, UV−vis absorptions of fresh and reacted catalysts were performed in diffuse reflectance mode. The results are shown in Figure 7a and b, respectively. On both fresh and reacted V_2O_5-loaded oxidized diamond catalysts, several broad absorption bands in the wavelength region of 200−600 nm are assigned to V^{5+} species in different dispersion states. These are ascribed to monomeric (243 and 315 nm) and oligomeric tetrahedrally coordinated V^{5+} species (360 nm) as well as square pyramidal (412 nm) and

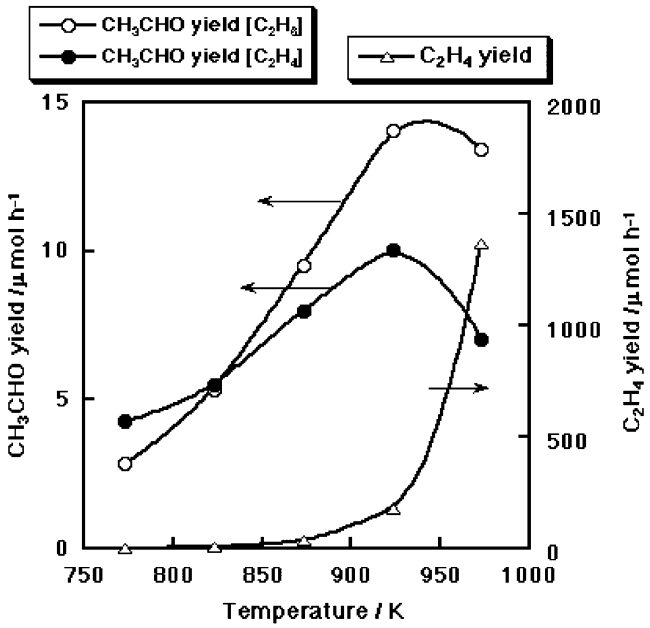

Figure 8. Partial oxidation of ethane or ethylene over V_2O_5 (3 wt %)/O-diamond. C_2H_6 (or C_2H_4)/CO_2 = 15:15 mL/mL, SV = 18 000 mL h^{-1} g of catalyst^{-1}. Flow rate = 30 mL/min, catalyst = 100 mg.

distorted octahedral V^{5+} species, which are probably due to absorbed water (458 nm). The catalyst that reacted under the CO_2 atmosphere exhibited very broad absorption in the region of 500−800 nm. This is assigned to the appearance of two bands of d−d transitions of V^{4+} (520 and 660 nm), indicating that the oxidation of C_2H_6 with CO_2 leads to the partial reduction of V^{5+} [43−50] to V^{4+}.[47−51]

Similar findings were observed in the dehydrogenation of ethylbenzene to styrene using the V_2O_5-loaded MgO catalyst, where V^{5+} in the fresh catalyst was reduced to lower valence state vanadium oxides even in the presence of CO_2.[31,32]

3.5. Reaction Pathway for the Production of CH_3CHO. In the course of the oxidation of C_2H_6 to CH_3CHO, a large amount of C_2H_4 was produced. The possibility of the oxidation of C_2H_4 to CH_3CHO was examined, and the result is illustrated in Figure 8. In a low-temperature range (773−823 K), the CH_3CHO yield showed similar tendencies in both C_2H_6 and C_2H_4 oxidation with CO_2 against the reaction temperature. However, the CH_3CHO yield in the oxidation of C_2H_4 was lower than that in the selective oxidation of C_2H_6 at higher temperatures of 873 to 973 K. In the selective oxidation of C_2H_6 using the V_2O_5-loaded oxidized diamond catalyst, C_2H_4 and H_2O were produced above 923 K, at which temperature the maximum yield of CH_3CHO was obtained. This clearly indicates that CH_3CHO production via C_2H_4 and CO_2 was not a necessary pathway in the selective oxidation of C_2H_6. The source of C_2H_4 seems to be the decomposition of CH_3CHO as shown in reaction 7. In addition, a small amount of CH_3CHO was produced at 773 K, but no C_2H_4 was observed. This result also indicates that CH_3CHO was not produced from ethylene through the dehydrogenation of C_2H_6. The decrease in the CH_3CHO yield at 973 K with C_2H_4 and CO_2 suggests that addition−elimination equilibrium might have controlled CH_3CHO production at an elevated temperature. In other words, a different intermediate could be considered between the reaction with C_2H_4 and C_2H_6.

$$CH_3CHO + H_2 \rightarrow C_2H_4 + H_2O \qquad (7)$$

The effect of the addition of a small amount of H_2O (partial pressure of 1.24 kPa) to the reaction system of C_2H_6 and CO_2

was examined. The addition of H_2O showed no effect except for a decrease in the yield of CH_3CHO at 973 K. This suggests that the following reaction (eq 8) can be neglected:

$$C_2H_4 + H_2O \rightarrow CH_3CHO + H_2 \quad (8)$$

4. Conclusions

(1) We have established a new root for the formation of CH_3CHO from C_2H_6 with CO_2 as an oxidant using an oxidized diamond supported vanadium oxide catalyst.

(2) The reaction of C_2H_6 over various vanadium oxide-loaded supports (Al_2O_3, Nb_2O_5, Ta_2O_5, GeO_2, SiO_2, and oxidized diamond) under an Ar flow did not give even a trace amount of CH_3CHO, indicating that CO_2 behaved as an oxidant.

(3) The lattice oxygen of vanadium oxide and oxygen on the diamond surface seems to transfer to C_2H_6 to give oxygenates, and oxygen atoms lost from the solid surfaces were supplied from CO_2.

(4) We propose the following reaction pathway: C_2H_6 was primarily transformed into CH_3CHO but not through C_2H_4, and HCHO was derived from the partial decomposition of CH_3CHO.

Acknowledgment. This work was supported by a Grant-in Aid for Exploratory Research (146553019) from the Ministry of Education, Science, Culture, Sports, and Technology of Japan. K.N. is grateful to JSPS for his young scientist fellowship.

References and Notes

(1) Oyama, S. T.; Somorjai, G. A. *J. Phys. Chem.* **1990**, *94*, 5022.
(2) Kobayashi, T.; Nakagawa, K.; Tabata, K.; Haruta, M. *J. Chem. Soc., Chem. Commun.* **1994**, 1609.
(3) Kobayashi, T.; Guilhaume, N.; Miki, J.; Kitamura, N.; Haruta, M. *Catal. Today* **1996**, *32*, 171.
(4) Teng, Y.; Kobayashi, T. *Chem. Lett*. **1998**, 327.
(5) Teng, Y.; Kobayashi, T. *Catal. Lett*. **1998**, *55*, 33.
(6) Nakagawa, K.; Teng, Y.; Zhao, Z.; Yamada, Y.; Ueda, A.; Suzuki, T.; Kobayashi, T. *Catal. Lett*. **1999**, *63*, 79.
(7) Zhao, Z.; Yamada, Y.; Ueda, A.; Sakurai, H.; Kobayashi, T. *Appl. Catal. A* **2000**, *196*, 37.
(8) Zhao, Z.; Yamada, Y.; Teng, Y.; Ueda, A.; Nakagawa, K.; Kobayashi, T. *J. Catal*. **2000**, *190*, 215.
(9) Zhao, Z.; Kobayashi, T. *Appl. Catal. A* **2001**, *207*, 391.
(10) Kobayashi, T. *Catal. Today* **2001**, *71*, 69.
(11) Yamada, Y.; Ueda, A.; Nakagawa, K.; Kobayashi, T. *Res. Chem. Intermed.* **2002**, *28*, 397.
(12) Uragami, Y.; Otsuka, K. *J. Chem. Soc., Faraday Trans*. **1992**, *88*, 3605.
(13) Burch, R.; Kieffer, R.; Ruth, K. *Top. Catal*. **1996**, *3*, 335.
(14) Tesser, L.; Bordes, E.; Gubelmann-Bonneau, M. *Catal. Today* **1995**, *24*, 335.
(15) Roy, M.; Gubelmann-Bonneau, M.; Ponceblanc, H.; Volta, J. C. *Catal. Lett*. **1996**, *42*, 93.
(16) Thorsteison, E. M.; Wilson, T. P.; Young, F. G.; Kasai, P. H. *J. Catal*. **1978**, *52*, 116.
(17) Iwamoto, M.; Taga, T.; Kagawa, S. *Chem. Lett*. **1982**, 1469.
(18) Mendelovici, L.; Lunsford, J. H. *J. Catal*. **1985**, *94*, 37.
(19) Iwamatsu, E.; Aika, K.; Onishi, T. *Bull. Chem. Soc. Jpn*. **1986**, *59*, 1665.
(20) Erdohelyi, A.; Solymosi, F. *Appl. Catal*. **1988**, *39*, L11.
(21) Erdohelyi, A.; Solymosi, F. *J. Catal*. **1990**, *123*, 31.
(22) Erdohelyi, A.; Solymosi, F. *J. Catal*. **1991**, *129*, 497.
(23) Erdohelyi, A.; Mate, F.; Solymosi, F. *J. Catal*. **1992**, *135*, 563.
(24) Wang, Y.; Otsuka, K. *J. Catal*. **1997**, *171*, 106.
(25) Nakagawa, K.; Okamura, M.; Ikenaga, N.; Suzuki, T.; Kobayashi, T. *Chem. Commun.* **1998**, 1025.
(26) Nakagawa, K.; Kajita, C,; Ide, Y.; Okamura, M.; Kato, S.; Kasuya, H.; Ikenaga, N.; Kobayashi, T.; Suzuki, T. *Catal. Lett.* **2000**, *64*, 215.
(27) Nakagawa, K.; Kajita, C.; Okumura, K.; Ikenaga, N.; Gamo, M. N.; Ando, T.; Kobayashi, T.; Suzuki, T. *J. Catal.* **2001**, *203*, 87.
(28) Kvylov, O. V.; Mamedov, A. Kh.; Mizabekova, S. R. *Stud. Surf. Sci. Catal.* **1994**, *82*, 159.
(29) Takahara, I.; Saito, M. *Chem. Lett*. **1996**, 973.
(30) Sugino, M.; Shimada, H.; Tsuda, T.; Miura, H.; Ikenaga, N.; Suzuki, T. *Appl. Catal. A* **1995**, *121*, 125.
(31) Sakurai, Y.; Suzaki, T.; Nakagawa, K.; Ikenaga, N.; Aota, H.; Suzuki, T. *Chem. Lett.* **2000**, 526.
(32) Sakurai, Y.; Suzaki, T.; Nakagawa, K.; Ikenaga, N.; Aota, H.; Suzuki, T. *J. Catal.* **2002**, *209*, 16.
(33) Nakagawa, K.; Kajita, C.; Ikenaga, N.; Kobayashi, T.; Gamo, M. N.; Ando, T.; Suzuki, T. *Chem. Lett*. **2000**, 1100.
(34) Nakagawa, K.; Nishimoto, H.; Enoki, Y.; Egashira, S.; Ikenaga, N.; Kobayashi, T.; Gamo, M. N.; Ando, T.; Suzuki, T. *Chem. Lett*. **2001**, 460.
(35) Nakagawa, K.; Hashida, T.; Kajita, C.; Ikenaga, N.; Kobayashi, T.; Gamo, M. N.; Suzuki, T.; Ando, T. *Catal Lett.* **2002**, *80*, 161.
(36) Suzuki, T.; Nakagawa, K.; Ikenaga, N.; Ando, T. *Stud. Surf. Sci. Catal.* **2002**, *143*, 1073.
(37) Nakagawa, K.; Kajita, C.; Ikenaga, N.; Suzuki, T.; Kobayashi, T.; Gamo, M. N.; Ando, T. *J. Phys. Chem. B* **2003**, *107*, 4048.
(38) Nakagawa, K.; Kajita, C.; Ikenaga, N.; Gamo, M. N.; Ando, T.; Suzuki, T. *Catal. Today* **2003**, *84*, 149.
(39) Ando, T.; Inoue, S.; Ishii, M.; Kamo, M.; Sato, Y.; Yamada, O.; Nakano, T. *J. Chem. Soc., Faraday Trans.* **1993**, *89*, 749.
(40) Ando, T.; Ishii, M.; Kamo, M.; Sato, Y. *J. Chem. Soc., Faraday Trans*. **1993**, *89*, 1383.
(41) Ando, T.; Ishii, M.; Kamo, M.; Sato, Y. *J. Chem. Soc., Faraday Trans.* **1993**, *89*, 1783.
(42) Ando, T.; Yamamoto, K.; Ishii, M.; Kamo, M.; Sato, Y. *J. Chem. Soc., Faraday Trans.* **1993**, *89*, 3635.
(43) Berndt, H.; Martin, A.; Bruckner, A.; Muller, D.; Kosslick, H.; Wolf, G.-U.; Lucke, B. *J. Catal*. **2000**, *191*, 384.
(44) Wokaun, A.; Schraml, M.; Baiker, A. *J. Catal*. **1989**, *116*, 595.
(45) Busca, G.; Lavalley, G. C. *Spectrochim. Acta, Part A* **1986**, *42*, 443.
(46) Schraml-Marth, M.; Wokaun, A.; Pohl, M.; Krauss, H.-L. *J. Chem. Soc., Faraday Trans.* **1991**, *87*, 2635.
(47) Ballhausen, C. J. *Introduction to Ligand Field Theory*; McGraw-Hill: New York, 1962.
(48) Centi, G.; Perathoner, S.; Trifiro, F.; Abouakais, A.; Aissi, C. F.; Guelton, M. *J. Phys. Chem*. **1992**, *96*, 2617.
(49) Morey, M.; Davidson, A.; Eckert, H.; Stucky, G. *Chem. Mater*. **1996**, *8*, 486.
(50) Landmesser, H.; Kosslick, H.; Storek, W.; Fricke, R. *Solid State Ionics* **1997**, *101*, 271.
(51) Busca, G.; Marchetti, L. J.; Centi, G.; Trifiro, F. *J. Chem. Soc., Faraday Trans*. **1985**, *81*, 1003.